# Preparation and Characterization of Elastomer-Based Nanocomposite Gels Using an Unique Latex Blending Technique

**Suman Mitra, Santanu Chattopadhyay, Anil K. Bhowmick***

*Rubber Technology Center, Indian Institute of Technology, Kharagpur, West Bengal 721302, India*

Received 29 December 2009; accepted 6 March 2010
DOI 10.1002/app.32389
Published online 13 May 2010 in Wiley InterScience (www.interscience.wiley.com).

**ABSTRACT:** Nanocomposite (NC) gels based on natural rubber (NR) and styrene butadiene rubber (SBR) were prepared by using a unique latex blending technique. These NC gels were prepared by first blending the water swollen unmodified montmorillonite clay ($Na^+$-MMT) suspension into the respective latices followed by prevulcanization to generate crosslinked nanogels. Use of water assisted fully delaminated $Na^+$-MMT suspension resulted in predominantly exfoliated morphology in the NC gels, as revealed by X-ray diffraction study and transmission electron microscopy. Addition of $Na^+$-MMT significantly improved various physical, mechanical and thermal properties of these NC gels. For example, 6 phr of $Na^+$-MMT loaded NR based NC gels registered 54% and 200% increase in tensile strength and Young's modulus, respectively, compared to the unfilled NR gels. SBR based NC gels also showed similar level of improvement in mechanical properties. Mechanical properties of NC gels prepared using this route were also compared with the NC gels prepared by co-coagulation and conventional curing technique and found to be superior. In the case of dynamic mechanical properties, NC gels showed higher glass transition temperatures along with a concomitant increase in storage moduli, compared to the unfilled gels. These $Na^+$-MMT reinforced NC gels also exhibited markedly improved thermal stability. © 2010 Wiley Periodicals, Inc. J Appl Polym Sci 118: 81–90, 2010

**Key words:** elastomers; latex blending; nanocomposites; gels; mechanical properties

## INTRODUCTION

Polymer-clay nanocomposites possess unique properties because of their nanometer sized features. The major advantages of nanocomposites over conventional composites include: lighter weight, improved mechanical properties,[1–3] ionic conductivity,[4] thermal resistance,[5] electrical conductivity,[6] and gas barrier properties[7,8] at low filler loading. The most common methods for the preparation of nanocomposites are solution blending, melt mixing, in situ polymerization, and latex compounding.[9,10]

Most of the rubbers, including natural rubber (NR) and styrene butadiene rubber (SBR) are available in the form of an aqueous dispersion of rubber particles, better known as latex. The layered silicates are also easily dispersed in water, as water acts as a swelling agent. This is due to the hydration of the intergallery cations of $Na^+$ or $K^+$. The water swelling ability of the natural clays depends upon the type of clay and its cation exchange capacity.[11] It has been reported in the literature that dilute aqueous suspension of montmorillonite clay can lead to full delamination of silicate layers.[12,13] The mixing of the latex along with the suspension of layered silicates followed by co-coagulation is a useful technique for generating rubber based nanocomposites, especially from the industrial application point of view. Many researchers have reported formation of rubber based nanocomposites from mostly montmorillonite clay with various rubbers like NR, SBR, acrylonitrile butadiene rubber (NBR), and carboxylated NBR following the above procedure.[14–20] However, in all the previous work, the crosslinking of the rubber nanocomposites has been carried out by following the conventional procedure in which the curing agents are mixed into the co-coagulated rubber-nanoclay mass and subsequently press cured at elevated temperature. As a result, substantial change in the morphology of the initial latex blended nanocomposite can not be ruled out after vulcanization. In fact, it has been reported in the literature that co-coagulation leads to considerable re-aggregation of individual silicate layers dispersed in the latex mixture.[15] At the same time, conventional mixing of

**Present address:* Indian Institute of Technology, Patna, Bihar 800013, India.
*Correspondence to:* A. K. Bhowmick (anilkb@rtc.iitkgp.ernet.in).
Contract grant sponsor: Council of Scientific and Industrial Research (CSIR); contract grant number: 9/81(715)/08-EMR-I.
Contract grant sponsor: Bridgestone Corporation, Japan.

**TABLE I**
**Prevulcanization Recipe and Designation of Different Nanocomposite Gels**

| Ingredients, parts (dry wt. basis) | Designation of nanocomposite gels | | | |
|---|---|---|---|---|
| | NS | $NSC_x$[a] | SBS | $SBSC_x$[a] |
| NR latex (60%) | 100.00 | 100.00 | – | – |
| SBR latex (30%) | – | – | 100.00 | 100.00 |
| 10% KOH | 0.25 | 0.25 | – | – |
| 50% aqueous dispersion of sulfur | 1.20 | 1.20 | 1.20 | 1.20 |
| 50% aqueous dispersion of ZDC | 1.20 | 1.20 | 1.20 | 1.20 |
| 50% aqueous dispersion of ZnO | 0.20 | 0.20 | 0.20 | 0.20 |
| $Na^+$-MMT (2% aqueous suspension) | – | 2–8[a] | – | 2–8[a] |

[a] '$x$' stands for the phr (parts per hundred parts of rubber) of $Na^+$-MMT used in the nanocomposite gels and has been varied from 2 phr to 8 phr, i.e., $x = 2$, 4, 6, and 8.

curing agents and subsequent press curing also contribute to the re-aggregation of silicate layers dispersed in the nanocomposite and lead to anisotropy in properties.[21]

In this present work, the authors have attempted to address the above issue by preparing dynamically cured latex nanocomposite gels, for the first time. We have also taken the advantage of water assisted pre-exfoliation of unmodified montmorillonite clay to form NR and SBR based nanocomposite gels. Aqueous suspension of pristine montmorillonite clay was mixed with NR and SBR latices at different concentrations. These latex blended nanocomposites were cured in latex stage itself, without coagulating the mass, by a prevulcanization technique using aqueous dispersion of curing agents. This has not been reported previously in the literature. In situ cured nanocomposite gels showed almost fully exfoliated morphology up to 6 phr of clay loading along with substantial improvements in mechanical and thermal properties. The results are expected to provide an understanding of the structure of nanocomposites prepared by the latex route, the relevant nano-compounding and curing mechanism for the formation of crosslinked nanocomposite gels. The procedure described herein may lead to the advent of much improved quality of industrial latex dipped products such as gloves and balloons, etc.

## EXPERIMENTAL

### Materials

High ammonia centrifuged natural rubber (NR) latex having 60% dry rubber content was procured from the Rubber Board, Kottayam, India. Sulfur, zinc oxide (ZnO), and zinc diethyl dithiocarbamate (ZDC), all in 50% aqueous dispersion, were also obtained from the same source and used as received. Styrene-butadiene rubber (SBR) latex having 30% total solid content and 30% bound styrene content was received from the Apar Industries, Ankeleswar, India. Cloisite® $Na^+$ ($Na^+$-montmorillonite, $Na^+$-MMT) clay was obtained from Southern Clay Products, Texas. Potassium hydroxide (KOH) was used as an emulsion stabilizer for NR during prevulcanization.

### Preparation of nanocomposite gels by unique latex blending technique

Aqueous suspension of Cloisite® $Na^+$ was prepared by dispersing the clay in water (2% w/v) with continuous stirring (700–800 rpm) for 72 h at ambient temperature (optimum time and concentration were determined from separate experiments). Aqueous suspension of $Na^+$-MMT clay and the rubber latex were mixed thoroughly and stirred for 2 h in a magnetic stirrer. After that, aqueous dispersions of the curing agents were added into it and the prevulcanization of the compounded latex-clay mixture was carried out at 80°C for 2 h under constant stirring (300–400 rpm). The clay concentration was kept at 2, 4, 6, and 8 phr, respectively. Table I reports the prevulcanization recipes used for the preparation of nanocomposite gels and their respective designation. Films of crosslinked nanocomposite gel were obtained from prevulcanized latex by casting on a flat glass plate and subsequent drying at ambient temperature (25 ± 2°C) to constant weight. Finally, the films were vacuum dried at 50°C for 12 h. These films were used for characterization of the nanocomposite gels.

### Preparation of nanocomposite gels by conventional latex blending technique

For comparison purpose, representative 6 phr Cloisite® $Na^+$ blended NR and SBR latex samples were subjected to co-coagulation followed by mixing and press curing. The latex-clay mixture was coagulated with dilute sulfuric acid (2%) and washed with water till acid free. Then the coagulated mass was dried in a vacuum oven at 50°C for 24 h. After that the dried rubber-clay mass was subjected to conventional mixing in a two-roll mill (Schwabenthan, Germany) for incorporation of various ingredients into them using the same recipe as tabulated in Table I.

Finally, the compounded mass was compression molded into a 1 mm thick sheet by curing till optimum cure time at 150°C in a David-Bridge hydraulic press (Castleton, Rocchdle, UK) at a pressure of 5 MPa. The molded sheet was used for tensile testing. In this work, conventionally cured 6 phr nanoclay filled NR and SBR NC gels were designated as $NSC_6$-CC and $SBSC_6$-CC, respectively.

## Characterization of nanocomposite gels

### Gel fraction and crosslink density measurements

Gel fraction (ratio of insoluble sample mass to initial sample mass) and crosslink density ($\upsilon$) of the NC gels as well as the control gels were determined from solvent swelling study by immersing the samples in toluene at room temperature (25 ± 2°C) for 48 h. The results reported here are the averages of five samples. Here, the initial sample mass in the case of NC gels refers to the nanocomposite gel mass (with nanoclays).

The well known Flory-Rehner equation was used to calculate the crosslink density.[22]

$$\upsilon = \frac{-1}{V}\left[\frac{\ln(1-v_r)+v_r+\chi_1 v_r^2}{v_r^{\frac{1}{3}}-\frac{v_r}{2}}\right] \quad (1)$$

where $\chi_1$ is the polymer–solvent interaction parameter, $V$, the molar volume of the solvent, and $\nu_r$, the volume fraction of the rubber in the swollen gel. The $\chi_1$ values for NR-toluene and SBR-toluene systems were taken as 0.35 and 0.31, respectively.[23] $\nu_r$ was calculated using the following equation:

$$v_r = \frac{(D_s - F_f A_w)\rho_r^{-1}}{(D_s - F_f A_w)\rho_r^{-1} + A_s \rho_s^{-1}} \quad (2)$$

where $D_s$, $F_f$, $A_w$, $A_s$, $\rho_r$ and $\rho_s$ are deswollen weight of the sample, fraction insoluble, sample weight, weight of the absorbed solvent corrected for swelling increment, density of rubber, and density of solvent, respectively.

### Dynamic light scattering

Dynamic light scattering (DLS) was carried out in Zetasizer Nano-ZS (Malvern Instrument, Worcestershire, UK) with a He-Ne laser of 632.8 nm wavelength. The data were analyzed by inbuilt machine software. The mean hydrodynamic particle diameter ($Z_{avg}$) was directly obtained from the machine software (as per ISO 13,321). Before testing, the latex samples were diluted to 0.1 g/L concentration level using doubly distilled water.

### X-ray diffraction

X-ray diffraction studies (XRD) were performed using a Philips X-Pert Pro MR-D diffractometer (Royal Philips Electronics, Amsterdam, The Netherlands) with Cu-target ($\lambda = 0.154$ nm) in the range 2–10° at a scanning rate of 0.5°/min. The acceleration voltage was 20 kV with 20 mA of beam current. The *d*-spacing of the clay particles was calculated using the Bragg's law.

### Transmission electron microscopy

The cast and dried nanocomposite gel samples for transmission electron microscopy (TEM) were prepared by ultracryomicrotomy using Leica Ultracut UCT, at around 40°C below the glass transition temperature of the compounds. Freshly cut glass knives with cutting edge of 45° were used to get the cryosections of 50 nm thickness. The microscopy was performed using JEM-2100 (JEOL, Tokyo, Japan) operating at an accelerating voltage of 200 kV. The morphology of NC gel particles immediately after prevulcanization was also studied using TEM. For this purpose, NC gel latex samples were diluted several times by using doubly distilled water, drop cast on copper grids, and dried in vacuum at 50°C for 24 h before testing.

### Tensile properties

For the measurement of tensile properties, dumbbell shaped specimens were punched out from the cast sheets as well as from the molded sheets of around 1mm thickness using ASTM Die-C. The tests were carried out as per the ASTM D 412–98 method in a Zwick Roell Z010 (Zwick Roell, Ulm, Germany), at a cross-head speed of 500 mm/min at 25 ± 1°C. The average of three tests is reported here.

### Dynamic mechanical measurements

Dynamic mechanical properties of the nanocomposite gels were measured as a function of temperature using the Dynamic Mechanical Analyzer DMA Q800 (TA Instruments, Luken's Drive, New Castle, DE). The measurements were taken under film-tension mode in the appropriate temperature range at a heating rate of 3°C/min at 1 Hz frequency. The peak value of Tan δ curves was taken as the glass transition temperature ($T_g$).

### Thermogravimetric analysis

Thermogravimetric analysis (TGA) of the nanocomposite gels was done using TA Instruments' (Luken's Drive, New Castle, DE) TGA-Q 50. The

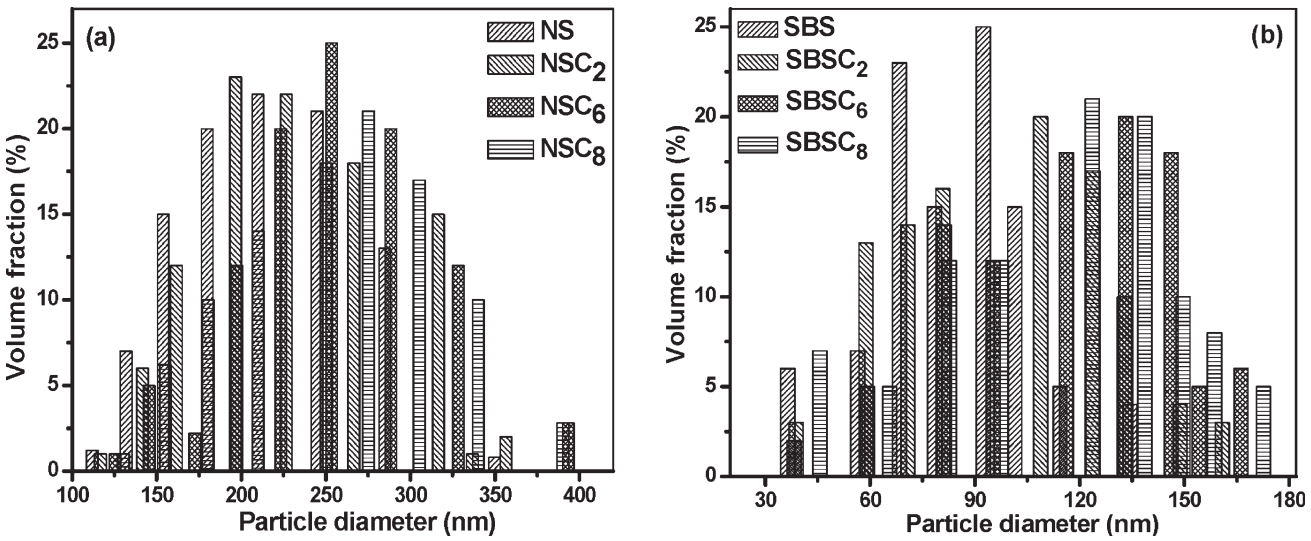


**Figure 1** PSD of nanocomposite gels by DLS (a) NR gels and (b) SBR gels.

samples (10 ± 2 mg) were heated from ambient temperature to 700°C in the furnace of the instrument under nitrogen atmosphere at a flow rate of 60 mL/min. The experiments were done at 10°C /min heating rate and the data of weight loss versus temperature were recorded online in the TA Instrument's Q series Explorer software.

## RESULTS AND DISCUSSION

### Particle size and crosslink density of nanocomposite gels

The nanocomposite gels were prepared by crosslinking the NR and SBR latices in presence of Cloisite® $Na^+$ using prevulcanization technique. The dynamic light scattering was effectively used to determine the particle size of gel particles and its distribution in control gels and their respective nanocomposites. Figure 1(a,b) shows the particle size distribution (PSD) of the NR and the SBR nanocomposite gels having 2, 6, and 8 phr of $Na^+$-MMT clay along with the respective NR and SBR gels. Both the NR and SBR nanocomposite gels show fairly broad PSD. In the case of NR gels and its nanocomposites, particle diameters range from 110 to 390 nm, with majority of the particles having sizes in the range of 200–300 nm [Fig. 1(a)]. Interestingly, addition of $Na^+$-MMT in the latex increases the particle diameters by about 30–40 nm and PSD shifts towards higher diameter and becomes broader compared to the control NS gel. This observation is well supported from the fact that the addition of clay in the latex considerably increases the mean hydrodynamic diameter ($Z_{avg}$), as reported in Table II. The SBR nanocomposite gels show a similar trend [Fig. 1(b)]. For example, control SBS gel has a $Z_{avg}$ of 92 nm, which increases to 130 nm in 8 phr clay containing SBR nanocomposite gel ($SBSC_8$). The increase in particle diameter in nanocomposite gels is believed to be due to the adsorption of clay layers on the latex particles and diffusion of some clay tactoids inside the latex particles.

As reported in Table II, the gel content and crosslink density values of the nanocomposite gels increase steadily over the control with the addition of $Na^+$-MMT clay up to 6 phr concentration, beyond which these level off. Although the increase in gel content is meager, crosslink density values show prominent rise with the addition of the nanoclays. There is about five-fold increase in crosslink density from NS to $NSC_6$, whereas it is almost three times in the case of $SBSC_6$ as compared to SBS. Crosslink density, as determined by solvent swelling method, essentially represents the sum of physical and chemical crosslinks. The polymer-nano clay interaction tremendously influences the amount of physical crosslinks, thereby increasing the overall crosslink density. Also, the presence of clay inside the matrix may greatly influence the extent of vulcanization.[24] Overall, the best result can be found with 6 phr of

**TABLE II**
**Properties of Nanocomposite Gels**

| Sample designation | Gel fraction (%) | Crosslink density × $10^4$ (gmol/cc) | $Z_{avg}$ particle diameter (nm) |
|---|---|---|---|
| NS | 94.2 | 0.75 | 219 |
| $NSC_2$ | 97.2 | 1.38 | 236 |
| $NSC_4$ | 98.0 | 2.95 | – |
| $NSC_6$ | 98.7 | 3.70 | 246 |
| $NSC_8$ | 98.5 | 3.63 | 250 |
| SBS | 92.5 | 1.50 | 92 |
| $SBSC_2$ | 94.4 | 2.71 | 112 |
| $SBSC_4$ | 95.5 | 3.29 | – |
| $SBSC_6$ | 97.1 | 4.18 | 127 |
| $SBSC_8$ | 96.8 | 4.15 | 130 |

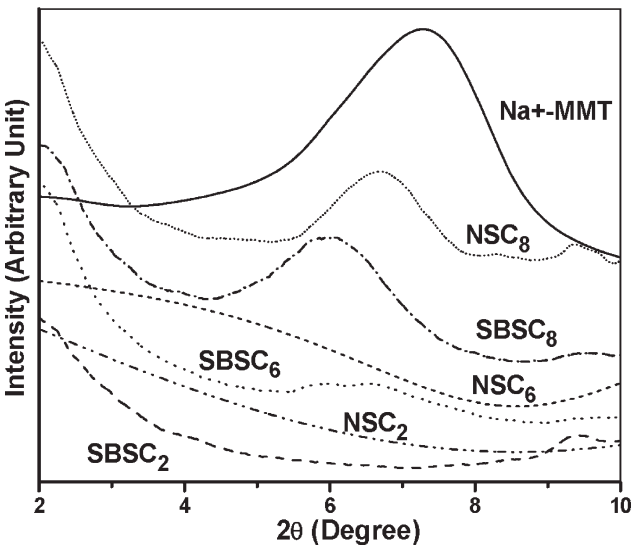


**Figure 2** XRD patterns of various nanocomposite gels.

$Na^+$-MMT loading for both NR and SBR nanocomposite gels, compared to the other three nanocomposite gels.

## Morphology of nanocomposite gels

### XRD analysis

The X-ray diffraction (XRD) pattern of Cloisite® $Na^+$ and its nanocomposite gels is shown in Figure 2. The pristine $Na^+$-MMT shows a peak at 7.5° corresponding to (001) basal plane reflections of silicate layers [$d_{001}$ = 1.17 nm]. There is no peak in the X-ray diffractograms of $NSC_2$, $NSC_6$, $SBSC_2$, and $SBSC_6$ indicating exfoliated or disordered intercalated morphologies up to 6 phr of clay loading. It is evident that the clay tactoids are well separated into platelets. In the case of $SBSC_8$ and $NSC_8$, a broad peak at lower angle (between 6° and 7°) compared to that of pristine $Na^+$-MMT can be observed. The $NSC_8$ shows a peak at 6.7° [$d_{001}$ = 1.35 nm] and $SBSC_8$ gives a peak at 6° [$d_{001}$= 1.45 nm]. It shows that the clay layers are intercalated by the polymer chains with larger *d*-spacing compared to that of the pristine clay, at relatively higher loading of clay. A similar observation is made with fluoroelastomer-based nanocomposites from unmodified $Na^+$-MMT clay prepared by a solution mixing process.[25] Apparently, the level of intercalation is greater in the case of the SBR nanocomposite gel, $SBSC_8$.

### TEM study

Two distinct types of morphologies are observed during the formation of these NC gels. The morphology of the representative $NSC_2$ and $SBSC_2$ gel particles in latex stage immediately after prevulcanization has been studied using TEM and these are presented in Figure 3(a,b), respectively. During the latex blending and subsequent prevulcanization stage, majority of $Na^+$-MMT platelets reside inside the latex particles. It can be seen clearly that individual nanoclay platelets are mostly housed inside the gel particles along with a few attached circumferentially in between the gel particles (indicated with arrows). Individual gel particles are spherical in shape, with most of them are in agglomerated state due to the method adopted for the preparation of TEM samples. Interestingly, once these NC latex gels are cast and dried, this type of morphology undergoes considerable transformation. The NC gel particles coalesce and form continuous matrix having exfoliated clay platelets which are described below.

Figure 4(a–d) illustrates the representative bright field TEM images of nanocomposite gels at 2 and 6 phr $Na^+$-MMT loadings. It is apparent that nanocomposite gels show predominantly exfoliated

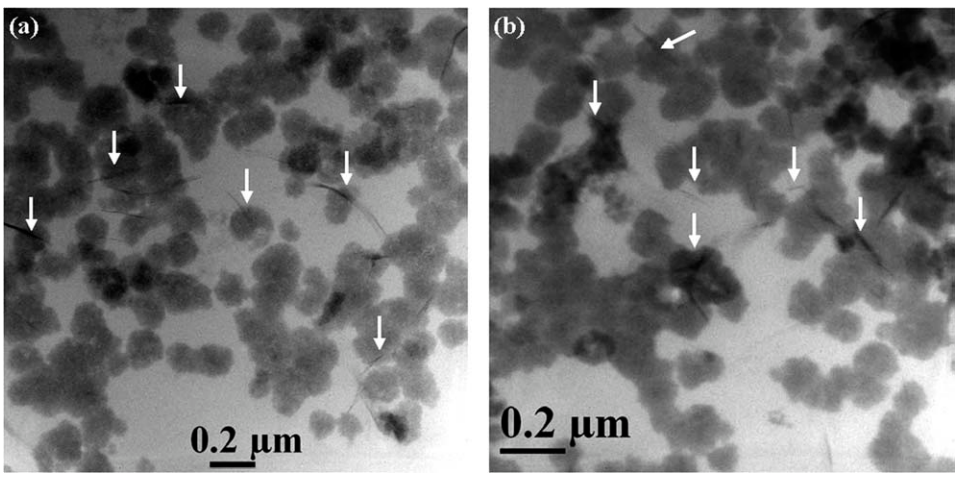


**Figure 3** Morphology of the unique latex blended NC gel particles as observed by TEM, (a) $NSC_2$ and (b) $SBSC_2$; the location of clay platelets inside the gel particles are shown by white arrows.

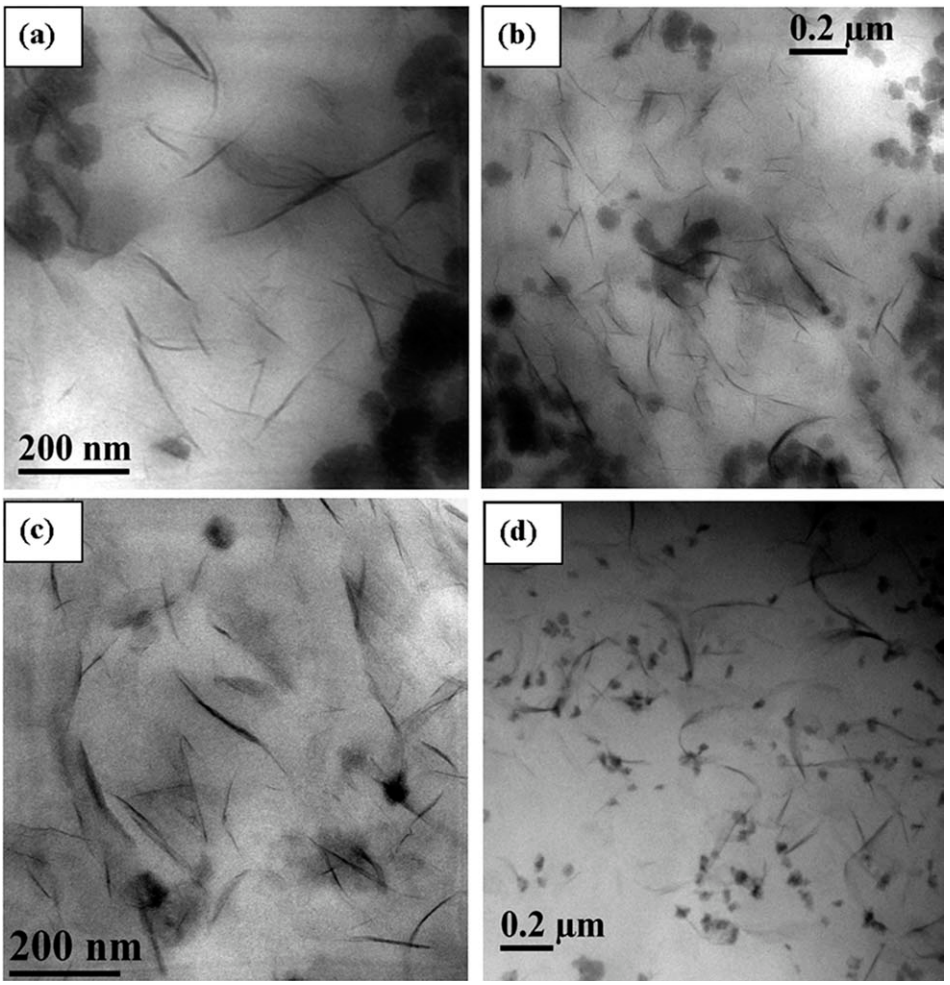


**Figure 4** Bright field TEM images of (a) $NSC_2$, (b) $NSC_6$, (c) $SBSC_2$, and (d) $SBSC_6$ (black circular dots are ZnO used for curing).

morphology. It can be noted here that the methodology followed to prepare the nanocomposite gel facilitates the formation of exfoliated clay structure. It has been reported in the literature that swelling of montmorillonite clay in water causes extensive delamination and breakdown of silicate layers.[12,13,15] In fact, it has been shown that $Na^+$-MMT disperse fully into the individual layers in its dilute aqueous suspension (clay concentration <10%).[15] This is due to the hydration of the intergallery cations of $Na^+$ or $K^+$ in montmorillonite clay, which is better known as innercrystalline swelling.[12] The nanocomposite gel formation, by the present method, has not altered the arrangements of dispersed clay layers, as seen from the TEM images. At 2 phr of $Na^+$-MMT loading, in both NR and SBR nanocomposite gels, well distributed individual clay platelets can be seen easily along with a few intercalated clay layers consisting of 2–3 clay platelets stacked together [Fig. 4(a,c)]. In the case of $NSC_6$ and $SBSC_6$, near fully exfoliated morphology is observed, with almost no sign of any clay particle agglomeration [Fig. 4(b,d)]. This type of morphology is responsible for the enhanced thermo-mechanical properties described later. The exfoliated morphology is a direct consequence of water assisted delamination of montmorillonite clay structure as described above. Hence, nanocomposite gels form predominantly exfoliated clay structure up to 6 phr of $Na^+$-MMT loading. It is interesting to note here that the SBR nanocomposite gels show higher level of exfoliation compared to the NR nanocomposite gels, as observed by both TEM and XRD. This may be due to the lower solid content of SBR latex (30%) used to prepare nanocomposite gels compared to the NR latex (60%), which facilitate the clay dispersion. At still higher loadings, the nanocomposite gels show some sign of clay particle–clay particle agglomeration (not shown here).

Conventional latex blending technique involving co-coagulation and subsequent press curing results in considerable agglomeration of the clay platelets as seen in Figure 5(a,b), for $NSC_6$-CC and $SBSC_6$-CC, respectively. Interestingly, the $Na^+$-MMT clay platelets

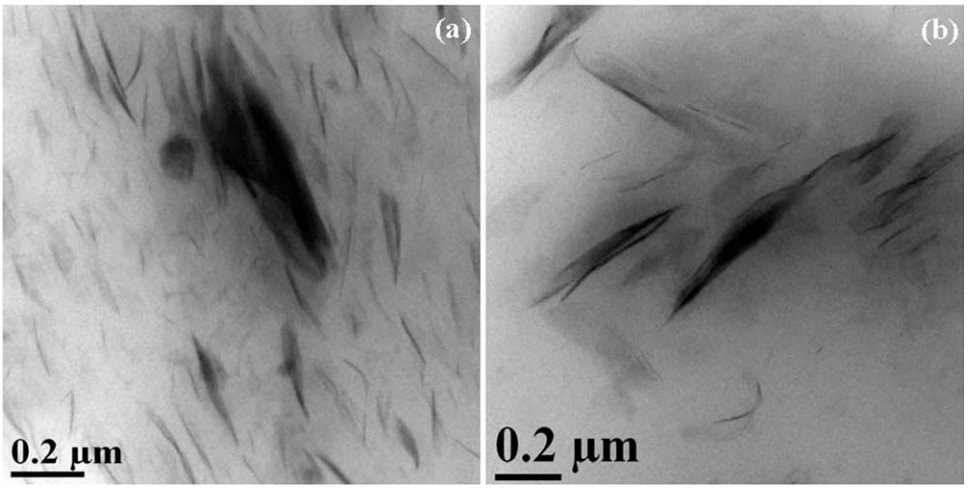


**Figure 5** Bright field TEM images of (a) $NSC_6$-CC and (b) $SBSC_6$-CC prepared by conventional latex blending technique.

are aligned in the molding /flow direction. It seems that conventional processing and subsequent press curing increases the tendency of re-agglomeration of clay platelets. It can be noted here that the advantage of using the pre-exfoliated clay suspension to form NC gels is partially suppressed after the conventional processing as evident from the evolved morphology. It has been also demonstrated in another study from our group that montmorillonite clay mixed with NR and SBR by conventional melt mixing technique does not lead to exfoliated morphology.[26,27] These present results will be very useful in the development of technology using NR/clay and SBR/clay nanocomposites.

## Properties of nanocomposite gels

### Tensile properties

The high levels of dispersion and exfoliation have a direct bearing on the mechanical properties of these nanocomposite gels. As shown in Figure 6(a,b), the tensile strength and Young's modulus register substantial increase with $Na^+$-MMT loading. For example, the values of tensile strength (TS) of $NSC_4$ and $NSC_6$ are 29% and 54%, respectively, higher than the control NS. In the case of SBR nanocomposite gels, the increase in Young's modulus ($Y_m$) is more than 147% for 8 phr clay loaded $SBSC_8$ over the unfilled one (SBS). While the Young's moduli show almost linear increase, the tensile strength gives a maximum at 6 phr of $Na^+$-MMT loading for both NR and SBR nanocomposite gels. The elongation at break values (EB) generate different trends for NR and SBR nanocomposite gels. In the NR nanocomposite gels, EB decreases consistently with the addition of $Na^+$-MMT [Fig. 6(a)], whereas in the case of SBR nanocomposite gels, EB increases steadily up to 6 phr clay loading and then falls off [Fig. 6(b)]. This has been attributed to the higher degree of exfoliation of nano clays in the SBR matrix. Sadhu and Bhowmick have reported similar observations from SBR and montmorillonite clay based nanocomposites prepared by solution mixing route.[28] The impressive level of improvement in the Young's moduli and the tensile strength of the nanocomposites can be

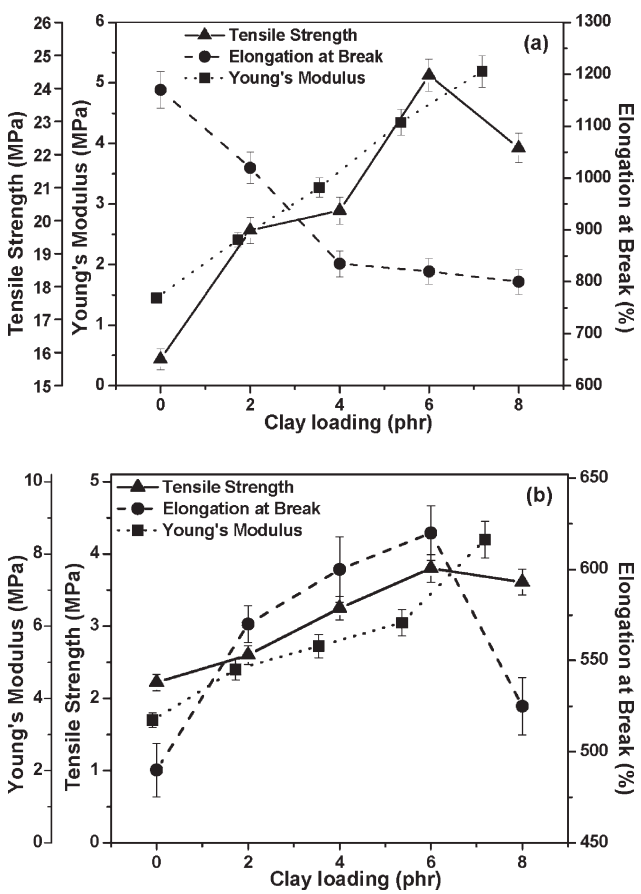


**Figure 6** Dependence of various tensile properties on clay loading for (a) NR gels and (b) SBR gels.

**TABLE III**
**Comparison of Different Properties of NC Gels Prepared by Unique Latex Blending Method and Co-Coagulation and Conventional Curing Technique**

| Sample designation | Tensile strength, TS (MPa) | Young's modulus, $Y_m$ (MPa) | Modulus at 300% elongation (MPa) | Elongation at break (%) | Volume fraction of rubber, $\nu_r$ | Storage modulus, $E'$ at 25°C (MPa) |
|---|---|---|---|---|---|---|
| NS | 15.80 | 1.45 | 1.30 | 1170 | 0.15 | 1.61 |
| $NSC_6$ | 24.40 (54%)[a] | 4.35 (200%) | 4.68 (260%) | 820 (−30%) | 0.28 (87%) | 31.50 |
| $NSC_6$-CC | 17.10 (8%) | 1.69 (17%) | 1.75 (35%) | 780 (−33%) | 0.20 (33%) | 12.68 |
| SBS | 2.20 | 3.40 | 1.55 | 490 | 0.19 | 1.53 |
| $SBSC_6$ | 3.80 (73%) | 6.10 (79%) | 1.77 (14%) | 620 (27%) | 0.27 (42%) | 20.00 |
| $SBSC_6$-CC | 2.30 (5%) | 3.67 (8%) | 1.64 (6%) | 550 (12%) | 0.22 (16%) | 8.73 |

[a] Figures in parenthesis indicate increment or decrement (negative values) in the respective properties over the control.

ascribed to the dispersed structure of clay at the nano level, the high aspect ratio, and the much improved polymer-filler interaction. The exfoliated morphology of the nanocomposite gels as evident from TEM and XRD is primarily responsible for the large enhancement in the mechanical properties. At relatively higher clay loading (>6 phr in the present case), due to reduction in the level of exfoliation and prevalence of nanoclay agglomeration, the mechanical strength drops significantly irrespective of the polymer matrix.

To compare the effectiveness of the present unique latex blending technique vis-à-vis conventional latex blending technique, representative 6 phr clay filled NR and SBR latex systems were coagulated, compounded, and press cured. Table III reports the tensile properties of the control gels and 6 phr $Na^+$-MMT loaded NC gels, prepared by unique latex blending and conventional latex blending techniques, for both NR and SBR. It is apparent that the NC gels formed by the present method show higher values of TS, $Y_m$ and modulus at 300% elongation compared to NC gels prepared by the conventional latex blending technique. In the case of TS, introduction of 6 phr $Na^+$-MMT by conventional technique results in meager 8 and 5% improvement for $NSC_6$-CC and $SBSC_6$-CC, respectively; compared to 54 and 73% increment for $NSC_6$ and $SBSC_6$, respectively, obtained by the present method. Similar trends are also observed for $Y_m$ and modulus at 300% elongation values (Table III). It has been shown earlier that conventional latex blending, due to coagulation and subsequent press curing steps, leads to considerable re-agglomeration of clay platelets (Fig. 5). As a result, reinforcement effect of individual (exfoliated) clay platelets is very much suppressed which leads to marginal improvement in tensile properties. On the other hand, unique latex blending technique employs curing in latex stage itself which results in better exfoliation of clay platelets (as evident from Fig. 4) and greater reinforcement in the resultant NC gels. This point is further substantiated from the $\nu_r$ values as tabulated in Table III. Better polymer-filler interaction in unique latex blended NC gels is responsible for higher values of $\nu_r$ compared to that of conventionally processed NC gels.

## Dynamic mechanical properties

Dynamic mechanical properties were measured to further elucidate the degree of filler-matrix interaction in the nanocomposite gels. The temperature dependence of tan δ for different nanocomposite gels is presented in Figure 7(a,b). In the case of NR based nanocomposite gels, significant shift in tan δ maxima towards higher temperature along with a noticeable reduction in tan δ peak height can be observed. The glass transition temperature, $T_g$, of the control NS is about −51°C, which increases to −46°C with the addition of 6 phr $Na^+$-MMT. Similarly, the peak height of tan δ curve decreases from 2.10 in NS to 0.53 for $NSC_8$. The SBR based nanocomposite gels show very similar trend. For example, the $T_g$ of SBS is −37°C, which changes to −28°C in $SBSC_6$, with the tan δ peak height reducing from 1.25 to 0.69. The increase in the $T_g$ and the reduction in the tan δ peak height with the addition of $Na^+$-MMT can be attributed to the enhanced polymer-nanoclay interaction, which results in restricted segmental mobility of the polymer chains. However, in both the cases, particularly for SBR nanocomposite gels, the $T_g$ remains unchanged or even shifts slightly towards the lower temperature with the increase in $Na^+$-MMT loading (beyond 6 phr). This is believed to be due to wall slippage of polymer chains against the clay and change of steric hindrance of bulky styrene groups.[27,28] The effect of $Na^+$-MMT on the storage modulus ($E'$) values of the nanocomposite gels is also compared in Figure 7(a,b) [as insets]. The moduli of the nanocomposite gels are much higher than those of the unfilled control NS and SBS gels, which further reflect the strong confinement of nano-dispersed silicate layers on the rubber chains. It can be mentioned here that the introduction of 6 phr $Na^+$-

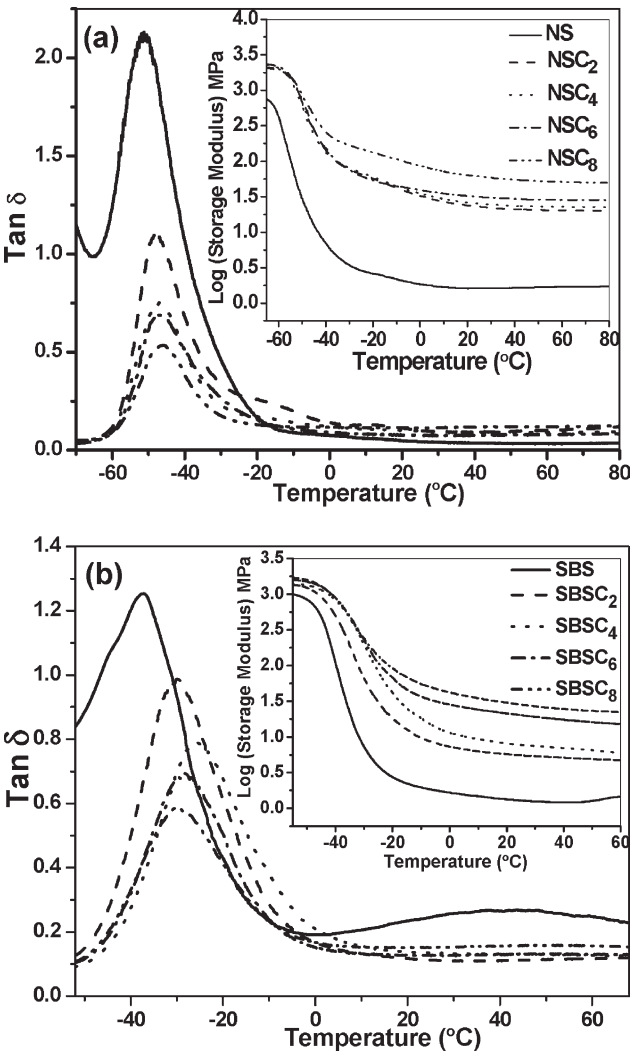


**Figure 7** DMA plots for (a) NR and (b) SBR based nanocomposite gels.

MMT in NR increases its storage modulus tremendously from 1.61 MPa to 31.50 MPa at 25°C, whereas in SBR, it is increased from 1.53 MPa to 20.00 MPa (Table III). It indicates that the elastic responses of neat gel matrix towards dynamic deformation are greatly influenced by the presence of nano-dispersed $Na^+$-MMT layers especially when these are completely exfoliated. Conventionally latex blended NC gels show much inferior $E'$ values, as seen in Table III, compared to those of the unique latex blended NC gels.

## Thermal properties

To examine the effect of clay dispersion on the thermal decomposition behavior of nanocomposite gels, thermo-gravimetric (TG) analyzes were performed as shown in Figure 8(a,b). These TG curves correspond to single-step degradation with well defined initial and final degradation temperatures. The results also show that the peak degradation temperature ($T_{max}$, the temperature corresponding to the maximum value in the derivative thermogram) shifts to the higher values with increasing $Na^+$-MMT loading, irrespective of the gel matrices used. A notable shift of $T_{max}$ by 25 and 11°C to higher temperature can be observed in the case of 8 phr $Na^+$-MMT clay filled SBR and NR nanocomposite gel samples, respectively. The enhancement in $T_{max}$ values is accompanied by a substantial reduction in peak degradation rate from 1.80%/°C in NS to 1.53%/°C in $NSC_8$ and 1.36%/°C in SBS to 1.23%/°C in the case of $SBS_8$, respectively, as shown in Figure 8(a,b) [insets]. The reduction in degradation rate, which is a measure of relative thermal stability, together with the increase in $T_{max}$, corresponds to better thermal stability in the nanocomposite gels compared to the

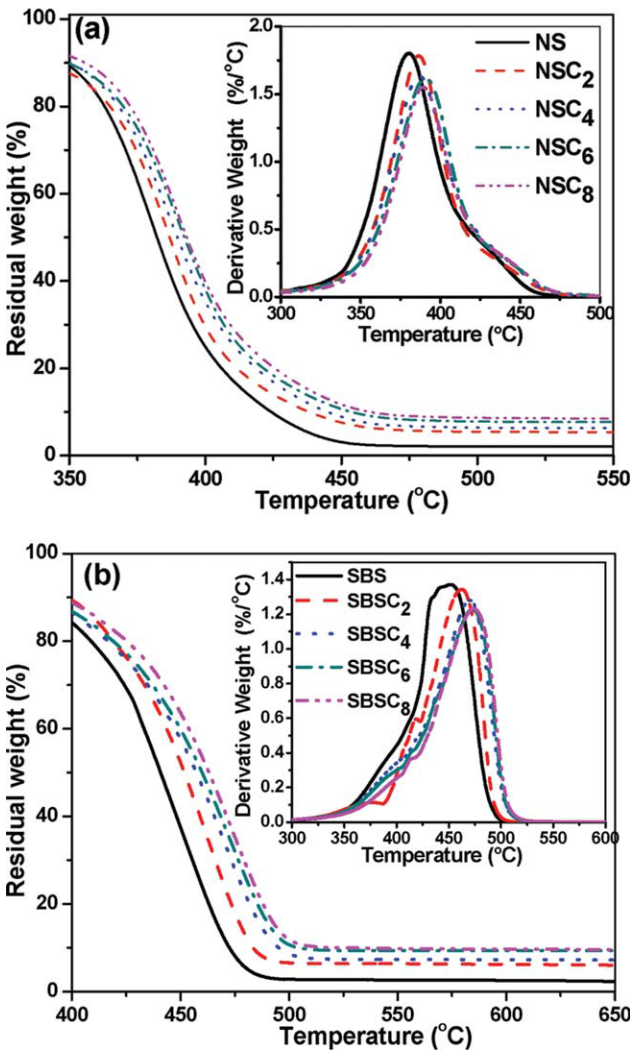


**Figure 8** TGA and DTG plots for (a) NR nanocomposite gels and (b) SBR nanocomposite gels. [Color figure can be viewed in the online issue, which is available at www.interscience.wiley.com.]

control gel. It has been reported that the thermal stability is a function of not only clay dispersion and polymer-filler interaction, but also clay content.[29] It is well-known that while the mechanical properties of the nanocomposites are directly related to dispersion of the clay in the polymer, the formation of a barrier hindering the mass transport of degrading polymer species and insulating the underlying polymer from the thermal source is responsible for higher thermal stability. Hence, the nanocomposite gels with relatively higher clay loadings have better thermal stability in contrast to the mechanical properties. Additionally, the formation of enhanced char yield in the high temperature region with increasing clay content also contributes to the enhancement of thermal stability.

## CONCLUSIONS

Unmodified montmorillonite clay based nanocomposite gels were prepared from NR and SBR latices using a latex blending and dynamic curing technique. Montmorillonite clay was swollen in water to assist exfoliation in the resulting nanocomposites. The particle size of the individual gel particle increased slightly with the formation of nanocomposite. The crosslink density of the nanocomposite gels was significantly higher than that of the unfilled gels. As prepared nanocomposite gels showed no peak in the XRD up to 6 phr clay loading, indicating substantial delamination of the clay platelets inside the gel matrix, and hence the existence of predominantly exfoliated morphology. This observation was well supported by the TEM study. At still higher clay loading, nanocomposite gels produced partially intercalated structure. The mechanical, dynamic mechanical, and thermal properties showed considerable improvement for both NR and SBR nanocomposite gels over the control gels. While the mechanical properties showed a maximum for 6 phr $Na^+$-MMT loaded nanocomposite gels, thermal stability increased steadily with the clay loading. The tensile properties of the NC gels formed by the present method were much higher compared to the NC gels prepared by the conventional latex blending technique. The overall enhancement in various properties was ascribed to the better dispersion and improved exfoliation of nanofillers in the gel matrix accomplished by the unique latex blending technique.

## References


1. Kojima, Y.; Usuki, A.; Kawasumi, M.; Okada, A.; Fukushima, Y.; Kurauchi, T.; Kamigaito, O. J Mater Res 1993, 8, 1185.
2. Lan, T.; Pinnavaia, T. J. Chem Mater 1994, 6, 2216.
3. Magaraphan, R.; Thaijaroen, W.; Lim-Ochakun, R. Rubber Chem Technol 2003, 76, 406.
4. Vaia, R. A.; Vasudevan, S.; Krawiec, W.; Scanlon, L. G.; Giannelis, E. P. Adv Mater 1995, 7, 154.
5. Lepoittevin, B.; Devalckenaere, M.; Pantoustier, N.; Alexandre, M.; Kubies, D.; Calberg, C.; Jerome, R.; Dubois, P. Polymer 2002, 43, 4017.
6. Zheng, W.; Wong, S. C. Compos Sci Technol 2003, 63, 225.
7. Messermith, P. B.; Giannelis, E. P. J Polym Sci Part A 1995, 33, 1047.
8. Gorrasia, G.; Tortora, M.; Vittoria, V.; Polletb, E.; Lepoittevin, B.; Alexandre, M.; Dubois, P. Polymer 2003, 44, 2271.
9. Sinha Ray, S.; Okamoto, M. Prog Polym Sci 2003, 28, 1539.
10. Pavlidou, S.; Papaspyrides, C. D. Prog Polym Sci 2008, 33, 1119.
11. Karger-Kocsis, J.; Wu, C. M. Polym Eng Sci 2004, 44, 1083.
12. Madsen, F. T.; Muller-Vonmoos, M. Appl Clay Sci 1989, 4, 143.
13. Katti, K. S.; Katti, D. R. Langmuir 2006, 22, 532.
14. Varghese, S.; Karger-Kocsis, J. Polymer 2003, 44, 4921.
15. Wu, Y. P.; Wang, Y. Q.; Zhang, H. F.; Wang, Y. Z.; Yu, D. S.; Zhang, L. Q.; Yang, J. Compos Sci Technol 2005, 65, 1195.
16. Wang, Y.; Zhang, L.; Tang, C.; Yu, D. J Appl Polym Sci 2000, 78, 1879.
17. Zhang, L.; Wang, Y.; Wang, Y.; Sui, Y.; Yu, D. J Appl Polym Sci 2000, 78, 1873.
18. Wu, Y. P.; Zhang, L. Q.; Wang, Y. Q.; Liang, Y.; Yu, D. S. J Appl Polym Sci 2001, 82, 2842.
19. Jia, Q. X.; Wu, Y. P.; Wang, Y. Q.; Lu, M.; Zhang, L. Q. Compos Sci Technol 2008, 68, 1050.
20. Alex, R.; Nah, C. J Appl Polym Sci 2006, 102, 3277.
21. Maiti, M.; Bhowmick, A. K. J Polym Sci B Polym Phys 2006, 44, 162.
22. Flory, P. J.; Rehner, J., Jr. J Chem Phys 1943, 11, 521.
23. Barton, A. F. M. Handbook of Polymer-Liquid Interaction Parameters and Solubility Parameters; CRC Press: New York, 1990; p 252, 353.
24. Bhattacharya, M.; Bhowmick, A. K. In Proceedings of the 174th Technical Meeting; American Chemical Society, Rubber Division: Louisville, KY, 2008; p 57/1–57/36.
25. Maiti, M.; Bhowmick, A. K. Comps Sci Technol 2008, 68, 1.
26. Bhattacharya, M.; Maiti, M.; Bhowmick, A. K. Rubber Chem Technol 2008, 81, 782.
27. Bhattacharya, M.; Maiti, M.; Bhowmick, A. K. Polym Eng Sci 2009, 49, 81.
28. Sadhu, S.; Bhowmick, A. K. J Appl Polym Sci 2004, 92, 698.
29. Maiti, M.; Mitra, S.; Bhowmick, A. K. Polym Degrad Stab 2008, 93, 188.